JOURNAL OF Materials CHEMISTRY

Sol–gel deposition of calcium silicate red-emitting luminescent films doped with Eu^{3+}

Qingguo Meng, Jun Lin, Lianshe Fu, Hongjie Zhang,* Shubin Wang and Yonghui Zhou

Key Laboratory of Rare Earth Chemistry and Physics, Changchun Institute of Applied Chemistry, Chinese Academy of Sciences, Changchun 130022, P. R. China.
E-mail: hongjie@ns.ciac.jl.cn; Fax: +86 431 5698041

Received 19th December 2000, Revised manuscript received 20th June 2001, Accepted 13th July 2001
First published as an Advance Article on the web 12th September 2001

Eu^{3+}-activated calcium silicate ($CaO–SiO_2:Eu^{3+}$) luminescent films were prepared by the sol–gel method. The structural evolution of the film was studied by X-ray powder diffraction (XRD), X-ray photoelectron spectroscopy (XPS) and scanning electron microscopy (SEM), and the luminescence properties of the phosphor films were investigated as a function of heat treatment temperature. The XRD study indicates that a kilchoanite phase forms in the film sintered at 800 °C, which is different from that in gel powder treated under the same conditions. The SEM results show that the film thickness decreases and the particles in the film become smaller with increasing heat treatment temperature. The $CaO–SiO_2:Eu$ film shows the characteristic emission of Eu^{3+} under UV excitation, with the Eu^{3+} $^5D_0\rightarrow{}^7F_2$ band (616 nm) being the most prominent. A large difference in the Eu^{3+} lifetime is observed between the film samples treated at 500 and 700 °C (or above). Concentration quenching occurs when the Eu^{3+} doping concentration is above 6 mol% of Ca^{2+} in the film.

Phosphor thin films are considered essential in high resolution devices such as cathode ray tubes, thin film electroluminescent panels, field emission displays and flat panel display devices.[1–3] Luminescent films show higher contrast, better lateral resolution and good thermal stability, as well as excellent adhesion to the substrate surface.[4] Representative examples include Y_2O_3 films doped with Eu^{3+}, which have been extensively studied as red-emitting phosphors.[5] There are many methods for the deposition of luminescent films, including pulsed laser deposition,[6] sputtering,[7] liquid phase epitaxy[8] and the sol–gel process.[9–13] The latter technique, which is suitable for the deposition of amorphous and crystalline thin films through dip- or spin-coating, has been extensively studied for applications in a variety of fields.[14]

Metal silicates have been widely reported as promising host materials for rare earth and transition metal ions with excellent luminescence properties in the blue, green and red spectral regions.[15] Mn^{2+}-activated zinc orthosilicate (Zn_2SiO_4) has been used as a green component in cathode ray tubes and electroluminescent devices because of its high luminescence efficiency and chemical stability.[1,16] Eu^{3+}-activated $CaSiO_3$ and $MgSiO_3$ gels and crystalline samples have been prepared by the sol–gel process and the effect of the sintering temperature on the luminescence properties of Eu^{3+} studied.[17,18] However, little attention has been paid to the preparation of luminescent silicate films *via* the sol–gel process.[19,20] The Eu^{3+} ion shows good luminescence performance in different bulk host materials and films,[21–24] and through the sol–gel method high quality thin films with good crystallinity and homogeneous composition can be obtained at a relatively low temperature. Therefore, in the present paper we report the deposition of $CaO–SiO_2:Eu^{3+}$ luminescent films *via* the sol–gel process, and investigate their microstructure and luminescence properties as a function of the annealing temperature and the Eu^{3+} doping concentration.

Experimental

Synthesis

The films were prepared by dipping quartz glasses of optical quality into precursor sols. The quartz substrates were precleaned in acid, followed by alkali, and then washed in ethanol. Finally, they were ultrasonically cleaned for 0.5 h in water to ensure that no residues remained.

Calcium nitrate, $Ca(NO_3)_2\cdot4H_2O$ (99.0%, A. R.; 0.014 mol), was pre-dissolved in 10 ml of ethanol and an equimolar amount of tetraethylorthosilicate (TEOS; C. P.) added under vigorous stirring. Hydrolysis took place upon addition of distilled water and the final molar ratio of TEOS : ethanol : water was 1 : 12 : 4. A small amount of HCl was added as a catalyst and the pH value of the mixture was adjusted to 2. Then the desired amount of europium nitrate, $Eu(NO_3)_3$ (0.2 M aqueous solution), was poured into the precursor solution. Highly transparent sols were obtained after stirring for a few hours, which were subsequently used for film deposition. Transparent gels could be obtained by drying the sols at 60 °C for 1 to 2 days.

The quartz glass substrates were dipped into the sols and withdrawn at a speed of 0.5 cm s^{-1}. The as-formed transparent films were dried at 120 °C to drive off any remaining solvent, then annealed to 500 °C slowly and held for an hour in air for densification. The final crack-free luminescent films were obtained by heat treatment between 500 and 1100 °C. The heating procedure is shown in Fig. 1. The same heating procedure was applied in the preparation of gel powders.

Characterization

A DT-30 Shimadzu thermal analyzer was used for recording thermogravimetric and differential thermal analysis (TG-DTA) curves for the $CaO–SiO_2:Eu^{3+}$ gel powders. The crystalline phase in the film samples was checked with a Rigaku D/max-II

DOI: 10.1039/b105963g

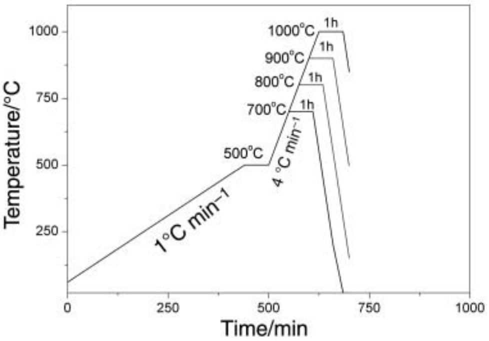

Fig. 1 The heating procedure for the preparation of CaO–SiO_2 : Eu^{3+} luminescent films.

B X-ray powder diffractometer using Cu-Kα ($\lambda = 0.15405$ nm) radiation. The XPS of the luminescent films was recorded on a VG ESCALAB MK II electron energy spectrometer using Mg-Kα (1253.6 eV) as the X-ray source. The surfaces and cross-sections of the films were inspected on a JEOL JXA-840 scanning electron microscope. The excitation and emission spectra were measured on a SPEX FL-2T2 spectrofluorimeter equipped with a 450 W xenon lamp as the excitation source (slit = 5 nm). Luminescence lifetimes were taken with a SPEX 1934D phosphorimeter using a 7 W xenon lamp as the excitation source with a pulse width of 3 μs. All the measurements were performed at room temperature.

Results and discussion

It was found that the transparency of the films depends upon the concentration of the coating solution and the sintering temperature. The films prepared from coating solutions containing 0.32 g ml^{-1} of $Ca(NO_3)_2$ were uniform, transparent and highly adherent to the substrate. Films are transparent when freshly deposited and become more or less opaque after sintering.

TG-DTA curves

Fig. 2 shows the TG-DTA curves of CaO–SiO_2 : 0.01Eu^{3+} gel powder dried at 60 °C in air at a heating rate of 10 °C min^{-1}. The endothermic peaks at 108 and 112 °C can be attributed to the evaporation of residual water and ethanol. The endothermic peaks at 429 and 530 °C, and the associated weight loss, result from the decomposition of the organic compounds and nitrates.[25] The weak exothermic peaks observed at 792 and 900 °C are due to the crystallization of the gel, as indicated by X-ray diffraction analysis results in the next section.

X-Ray powder diffraction

Fig. 3 presents the XRD patterns of CaO–SiO_2 : 0.01Eu^{3+} (molar ratio of Eu/Ca is 1 mol%) films heat treated at 700, 800, 900 and 1100 °C. No apparent diffraction peak is observed in the XRD pattern of the film sample heated at 700 °C. The broad peak at $2\theta = 21°$ is due to the amorphous phase of the silica glass substrate. Further heating at 800 and 900 °C leads to the formation of the crystalline phase of kilchoanite (JCPDS Card 29-370), as indicated by the presence of two diffraction peaks at $2\theta = 30.8$ and 29.4°. These two peaks are assigned to the (116) and (310) reflections of the kilchoanite phase $Ca_6(SiO_4)(Si_3O_{10})$, respectively. It is clear that the peak intensity increases with increasing temperature, suggesting improvements in crystallinity. The presence of the kilchoanite phase, which is different from the bulk gel glass, is probably due to the two-dimensional structure of luminescent films.[18] Finally, firing at 1100 °C leads to the disappearance the two kilchoanite phase peaks and causes a new weak peak at $2\theta = 30.1°$ to appear in the XRD pattern. This peak is assigned to the (320) diffraction plane of the wollastonite phase (JCPDS Card 27-88). The phase transition from kilchoanite to wollastonite is due to the reaction of kilchoanite with the SiO_2 substrate at high temperature (1100 °C): $Ca_6(SiO_4)(Si_3O_{10})$ (kilchoanite) + $2SiO_2 \rightarrow 2Ca_3Si_3O_9$ (wollastonite).

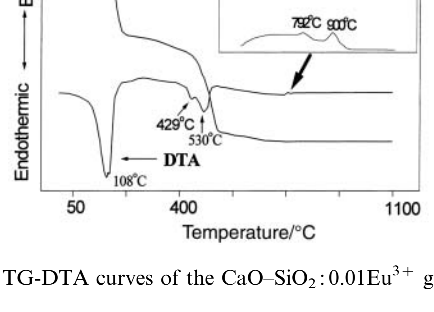

Fig. 2 TG-DTA curves of the CaO–SiO_2 : 0.01Eu^{3+} gel powder.

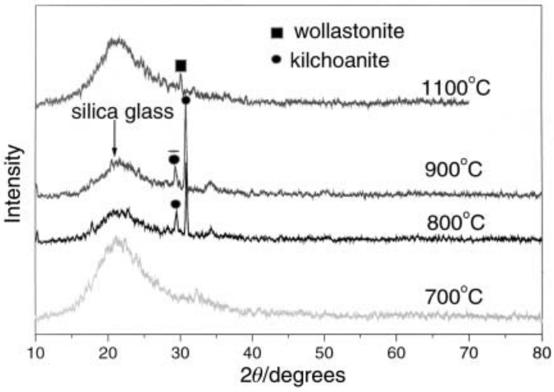

Fig. 3 XRD patterns of CaO–SiO_2 : 0.01Eu^{3+} luminescent films annealed at different temperatures.

Surface analysis

The morphology of the CaO–SiO_2 : Eu^{3+} films was investigated by SEM. SEM images of the surfaces and cross-sections of the luminescent films recorded at 5000 × and 1000 × magnification are shown in Fig. 4. In the sample sintered at 500 °C, the grains remain aggregated and irregularly shaped, while at 800 °C the particles become homogenous and well distinguished with spherical shapes and diameters of 2.0–3.0 μm. Sintering at even higher temperature (1050 °C) reduces the grain diameter to 1.0–2.0 μm. The film thickness can be seen clearly from the SEM images of the cross-sections of the films [Fig. 4(b)]. The films are uniform in thickness across the substrate; the film treated at 500 °C is about 10.0 μm thick. With increasing sintering temperature, the film becomes thinner. The films treated at 800 and 1050 °C are 7.0 and 3.0 μm thick, respectively. Three kinds of physicochemical process may occur in the course of the heat treatment of the sol–gel film.[26] Following the first process, the release of water and residual organic groups, as indicated by TG-DTA curves, the second process is characterized by collapse of the host skeleton, which causes the film to shrink. Hence, the films become thinner with increasing temperature. The final process is the crystallization of the film (as shown in the XRD patterns), which causes the grains in the film to become smaller.

XPS analysis

The atomic composition and the chemical state of the atoms in the film were analyzed by XPS. Signals from Si, Ca and O are

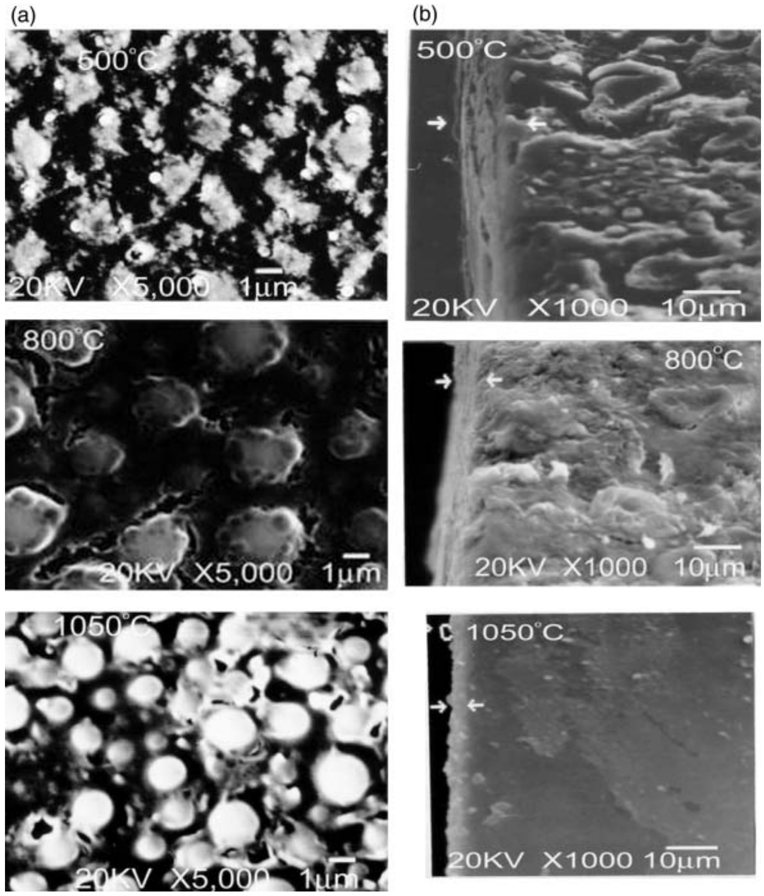

Fig. 4 SEM micrographs of the surfaces (a) and cross-sections (b) of CaO–SiO_2 : 0.01Eu^{3+} luminescent films heated at different temperatures.

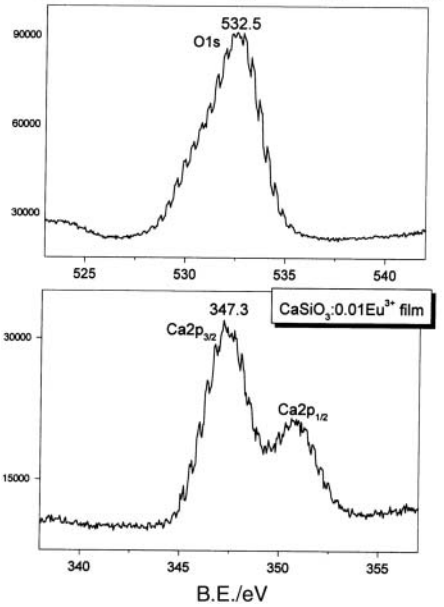

Fig. 5 XPS patterns of CaO–SiO_2 : 0.01Eu^{3+} luminescent film sintered at 1100 °C.

observed in the XPS of the luminescent film between 90 to 542 eV, but the Eu 4d peak is not detected because of its low concentration in the film. The XPS peaks corresponding to the Si 2p, O1s, and Ca $2p_{3/2}$ and $2p_{1/2}$ core levels of the sample are shown in Fig. 5, and the results of atomic composition and the chemical state analysis are summarized in Table 1. The data from our film samples in Table 1 are in good agreement with those in the literature, confirming further the formation of the wollastonite phase at 1100 °C.

Photoluminescence properties

The excitation and emission spectra of CaO–SiO_2 : 0.01Eu^{3+} luminescent film heat treated at 800 °C are shown in Fig. 6. The excitation spectrum obtained by monitoring the Eu^{3+} $^5D_0 \rightarrow {}^7F_2$ emission at 616 nm consists of a broad band centered at 250 nm and a number of narrow excitation peaks, with the strongest one peaking at 394 nm. The broad band is attributed to charge transfer (CT) between the Eu^{3+} and the surrounding

Table 1 Atomic composition and chemical state of CaO–SiO_2 : 0.01Eu^{3+} film annealed at 1100 °C determined by XPS analysis

		XPS Peak binding energy/eV		
Element	XPS Peak	This work	References	
Ca	Ca $2p_{3/2}$	347.3	$Ca_3Si_3O_9$	347.04[a]
Si	Si 2p	103.0	wollastonite	102.16[a]
			wollastonite	102.36[b]
O	O 1s	532.5	wollastonite	531.4[b]

[a] J. Wang, W. Wu and D. Feng, *Introduction to Electron Energy Spectroscopy*, National Defence Industry Press, Beijing, 1992. [b] C. D. Wagner, D. E. Kinisky, H. A. Six, W. T. Jansen and J. A. Taylor, *J. Vac. Sci. Technol.*, 1982, **21**, 933.

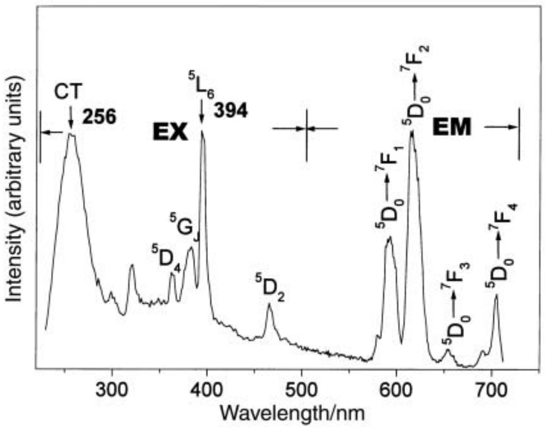

Fig. 6 Excitation ($\lambda_{em}=616$ nm) and emission ($\lambda_{ex}=256$ nm) spectra of CaO–SiO$_2$: 0.01Eu^{3+} luminescent film heated at 800 °C.

O^{2-} ions, while the lines are due to f–f transitions within the Eu^{3+} $4f^6$ configuration. The emission spectrum excited at the CT band contains main emission peaks corresponding to the $^5D_0\rightarrow{}^7F_j$ ($j=0, 1, 2, 3, 4$) transitions of Eu^{3+}, with the hypersensitive $^5D_0\rightarrow{}^7F_2$ red emission being the most prominent.

Fig. 7(a) gives the excitation spectra of CaO–SiO$_2$: 0.01Eu^{3+} luminescent films after sintering at different temperatures. It is known from Fig. 7(a) that the excitation spectra of samples heated at 700 and 800 °C are similar but extensive changes occur after heat treatment at 1000 °C and above. The excitation intensity (measured by the relative height) of the CT transition is nearly the same as that of the transition $^7F_0\rightarrow{}^5L_6$ (394 nm) for film samples sintered at 700 and 800 °C, while the CT transition increases and the $^7F_0\rightarrow{}^5L_6$ transition decreases in intensity for the samples sintered at 1000 and 1100 °C. Here we use R ($R=I_{CT}/I_{394}$) to show the change in the excitation intensity, where I_{CT} is the intensity of CT excitation and I_{394} is the intensity of the $^7F_0\rightarrow{}^5L_6$ transition. Table 2 lists the values of R at each sintering temperature employed. Clearly, a dramatic increase in R and a red shift of the CT band can be observed on moving from lower temperature (700 and 800 °C) to higher temperature (1000 and 1100 °C) treated luminescent films in Table 2 and Fig. 7(a), respectively. The main factor affecting the intensity of the CT band is the efficiency of the energy transfer process from the CT band to the Eu^{3+} emitting level. With increasing heat treatment temperature of the luminescent films, the interaction between O^{2-} and Eu^{3+} ions in the silicate host becomes stronger. This is probably due to the fact that the electron transfer from O^{2-} to Eu^{3+} becomes easier (*i.e.* the CT band of Eu^{3+}–O^{2-} shifts to lower energy), which further increases the overlap between the Eu^{3+} CT band and the emitting levels of Eu^{3+}. That is to say, the efficiency of the energy transfer process from the CT band to the Eu^{3+} emitting level increases. This is why increasing R values and a red shift of the CT band are observed when comparing the lower temperature (700 and 800 °C) to the higher temperature (1000 and 1100 °C) treated samples. Weak interactions between Eu^{3+} and O^{2-} in gel make the excitation line at 394 nm much stronger.[18]

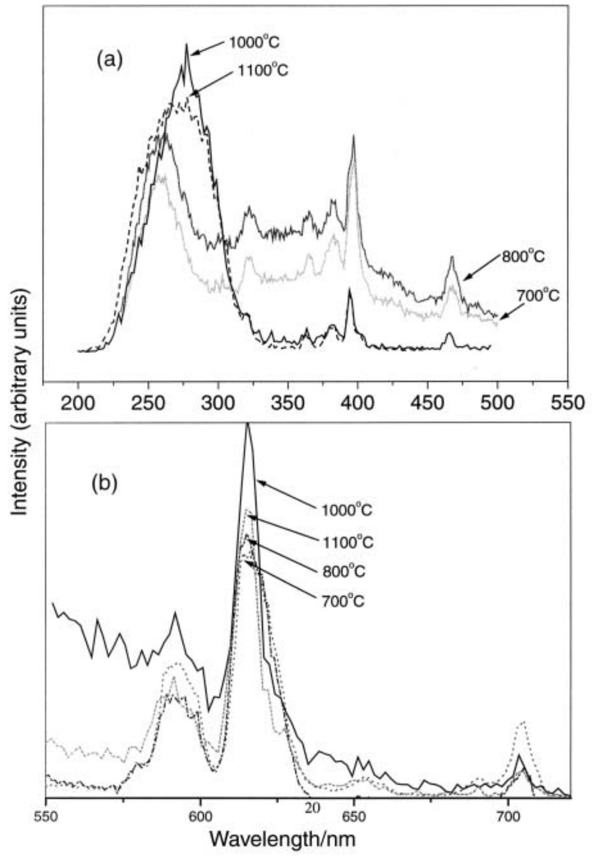

Fig. 7 Effect of heating temperature on excitation ($\lambda_{em}=616$ nm) (a) and emission ($\lambda_{ex}=256$ nm) (b) spectra of CaO–SiO$_2$: 0.01Eu^{3+} luminescent films.

Table 2 Dependence of R ($R=I_{CT}/I_{394}$) on the heat treatment temperature

Heat treatment temperature/°C	R
700	0.944
800	1.020
1000	5.022
1100	4.182

The emission spectra of CaO–SiO$_2$: Eu^{3+} film as a function of heat treatment temperature from 700 to 1100 °C are presented in Fig. 7(b). It can be seen from this figure that the Eu^{3+} emission intensity increases with increasing heat treatment temperature up to 1000 °C, which agrees with the improvement in the crystallinity with increasing sintering temperature, as shown in the XRD patterns (Fig. 3). The emission intensity of the sample heated at 1100 °C decreases slightly from that of the 1000 °C, which is probably due to the phase transition.

The effect of heat treatment temperature on the photoluminescence decay curves of the $^5D_0\rightarrow{}^7F_2$ red emission of CaO–SiO$_2$: 0.01Eu^{3+} films and powders are shown in Fig. 8(a) and (b), respectively. Basically, all these decay curves can be fitted into a single exponential function as $I=A+I_0\exp(-\tau/t)$ (where A is a constant and τ is the lifetime), and the lifetime values derived from this fitting are shown in the figures. It can be seen from Fig. 8 that the fluorescence lifetimes of Eu^{3+} increase with increasing heat treatment temperature both in the thin film and powder samples. This is due to the reduction of OH groups on heating. Many studies have shown that the fluorescence lifetime of the Eu^{3+} ion is sensitive to the presence of OH oscillators and that the rate of non-radiative de-excitation of the Eu^{3+} $^5D_0$ level is directly proportional to the number of OH oscillators. The lifetime of Eu^{3+} increases by a factor of five on moving from 500 (0.68) to 700 °C (3.20 ms) treated film samples [Fig. 8(a)], due to the elimination of OH groups. But on moving from 700 to 900 °C sintering, the lifetimes show no apparent increase in the film samples, indicating that the elimination of OH groups is nearly complete at 700 °C.[26] However, the Eu^{3+} lifetimes increase steadily from 500 (1.21) to 900 °C (1.87 ms) in the gel powder samples [Fig. 8(b)]. It has been reported that a certain amount of OH groups still exist in powder samples annealed at temperatures

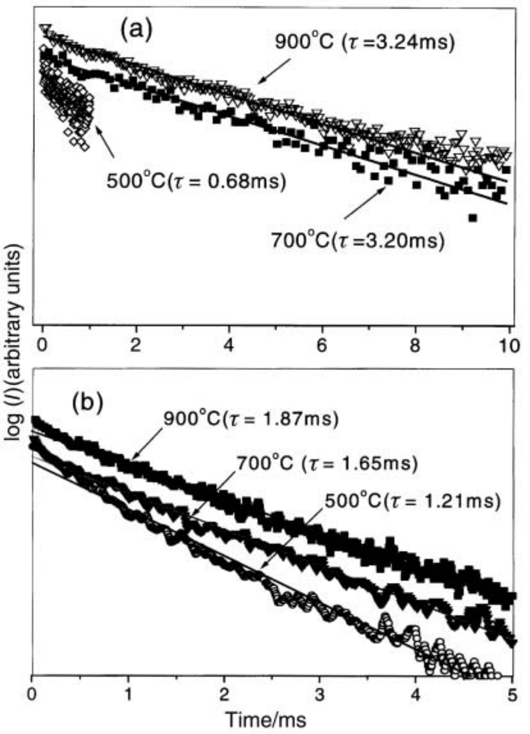

Fig. 8 Photoluminescence decay curves of the Eu^{3+} $^5D_0 \rightarrow {}^7F_2$ red emission in $CaO–SiO_2:0.01Eu^{3+}$ films (a) and gel glasses (b) at different annealing temperatures.

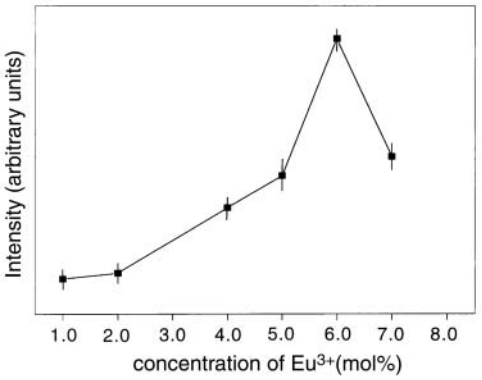

Fig. 9 Dependence of the relative emission intensity of Eu^{3+} on its doping concentration.

above 1000 °C.[27] Due to a longer migration distance for water in gel glasses compared to films, the water molecules are more difficult to release in gel powders. Hence, the different behavior of the lifetime as a function of temperature in the film and powder samples can be understood.

Fig. 9 shows the dependence of the relative emission intensity of Eu^{3+} ($^5D_0 \rightarrow {}^7F_2$ transition at 616 nm) on its molar concentration in the films sintered at 800 °C. The Eu^{3+} emission intensity first increases with doping concentration, reaching a maximum value when the concentration of Eu^{3+} is 6 mol% of that of Ca^{2+}, and then decreasing sharply with increasing Eu^{3+} concentration due to the concentration quenching effect. It is well known that a very efficient energy transfer occurs among activator ions at high concentrations. The probability of energy transfer to a similar nearby ion can be very much greater than the probability of radiative decay, so that the excitation moves about among the ions and may ultimately be trapped at a sink and dissipated as heat.[28]

Conclusion

$CaO–SiO_2:Eu^{3+}$ red-emitting luminescent films can be synthesized by the sol–gel method; the films become thinner and their constituent particles become smaller with increasing annealing temperature. The crystalline phase is kilchoanite between 800–900 °C in the $CaO–SiO_2:Eu^{3+}$ film, which changes to wollastonite at 1100 °C due to reaction with the silica glass substrate. The excitation and emission intensity and the fluorescent lifetime of Eu^{3+} in the films increase with increasing heat treatment temperature. Elimination of OH groups in the films is nearly complete at 700 °C. Concentration quenching occurs when the Eu^{3+} doping concentration is above 6 mol% of Ca^{2+} in the film.

Acknowledgements

This work is financially supported by the "973" National Key Project for Fundamental Research, the National Natural Science Foundation of China (no. 29731010 and 29971030), the Noble Youth Fund of Natural Science (no. 29225102) and "Bairen Jihua"of the Chinese Academy of Sciences.

References

1 X. Ouyang, A. H. Kitai and T. Xiao, *J. Appl. Phys.*, 1996, **79**, 3229.
2 G. A. Hirata, J. Mckittrick, M. Avalos-Borja, J. M. Siquetros and D. Devlin, *Appl. Surf. Sci.*, 1997, **113**, 509.
3 S. L. Jones, D. Kumar, R. K. Singh and P. H. Holloway, *Appl. Phys. Lett.*, 1997, **71**, 404.
4 L. Z. Meznar, B. Pracek, B. Orel and P. Bukovec, *Thin Solid Films*, 1998, **317**, 336.
5 K. G. Cho, D. Kumar, P. H. Holloway and R. K. Singh, *Appl. Phys. Lett.*, 1998, **73**, 3508.
6 X. W. Sun and H. S. Kwok, *Appl. Phys. A: Solid Surf.*, 1999, **69**, S39.
7 J. Shmulovich and D. F. Kocian, *SID Int. Symp. Digest Technol. Pap.*, 1989, 297.
8 J. M. Robertson and M. W. van Tol, *Thin Solid Films*, 1984, **14**, 221.
9 C. Strohhöfer, J. Fick, H. C. Vasconcelos and R. M. Almeida, *J. Non-Cryst. Solids*, 1998, **226**, 182.
10 M. Almeida Rui, X. M. Du, D. Barbier and X. Orignac, *J. Sol-Gel. Sci. Technol.*, 1999, **14**, 209.
11 R. P. Rao, *Solid State Commun.*, 1996, **99**, 439.
12 D. Ravichandran, R. Roy, A. G. Chakhovskoi, C. E. Hunt, W. B. White and S. Erdei, *J. Lumin.*, 1997, **71**, 291.
13 N. J. Hess and G. J. Exarhos, *J. Non-Cryst. Solids*, 1994, **178**, 91.
14 S. Sakka, *Struct. Bonding*, 1996, **85**, 1.
15 D. E. Harrison and V. Hoffman, *J. Electrochem. Soc.*, 1959, **106**, 800.
16 N. Yocom, R. S. Meltzer, K. W. Jang and M. G. Rim, *Inf. Disp.*, 1996, **4**, 169.
17 X. P. Fan, M. Q. Wang, Y. Yu and Q. Z. Wu, *J. Phys. Chem. Solids*, 1996, **57**, 1259.
18 X. P. Fan, M. Q. Wang, Z. L. Hong and G. D. Qian, *J. Phys: Cond. Mater*, 1997, **9**, 3479.
19 J. Lin, D. U. Sänger, M. Mennig and K. Bärner, *Thin Solid Films*, 2000, **360**, 39.
20 H. X. Zhang, C. H. Kam, Y. Zhou, X. Q. Han, S. Buddhudu, Y. L. Lam and C. Y. Chan, *Thin Solid Films*, 2000, **370**, 50.
21 A. M. Srivastava, *J. Lumin.*, 1996, **69**, 301.
22 M. Dejneka, E. Snitzer, R. E. Riman, Y. Gao and C. S. Shi, *J. Phys. Chem. Solids*, 1996, **57**, 1303.
23 R. Ternane, M. Trabelsi-Ayedi, N. Kbir-Ariguib and B. Piriou, *J. Lumin.*, 1999, **81**, 165.
24 R. Reisfeld, M. Zelner and A. Patra, *J. Alloys. Compd.*, 2000, **300–301**, 147.
25 Takashi Hayashi and Hajime Saito, *J. Mater. Sci.*, 1980, **15**, 1971.
26 X. M. Du and R. M. Almeida, *J. Sol-Gel. Sci. Technol.*, 1997, **8**, 377.
27 E. J. A. Pope and J. D. Mackenzie, *J. Am. Ceram. Soc.*, 1993, **76**, 1325.
28 *Luminescence Spectroscopy*, ed. M. D. Lumb, Academic Press, New York, 1978.